C. R. Palevol 12 (2013) 223–231

Contents lists available at SciVerse ScienceDirect

Comptes Rendus Palevol

www.sciencedirect.com

Human palaeontology and prehistory

The functionally-related signatures characterizing the endostructural organisation of the femoral shaft in modern humans and chimpanzee

Les signatures fonctionnelles caractérisant l'organisation endostructurale de la diaphyse fémorale chez les humains modernes et le chimpanzé

Laurent Puymerail [a,b,*]

[a] *Unité d'anthropologie bio-culturelle, « Droit, éthique & santé » (ADÉS), UMR 7268, université d'Aix-Marseille–EFS–CNRS, faculté de médecine – secteur nord, CS 80011, boulevard Pierre-Dramard, 13344 Marseille cedex 15, France*
[b] *Département de préhistoire, Muséum national d'histoire naturelle, UMR 7194, 75005 Paris, France*

ARTICLE INFO

Article history:
Received 1st November 2012
Accepted after revision 10 April 2013
Available online 14 June 2013

Presented by Yves Coppens

Keywords:
Locomotion
Femoral shaft
Inner structure
Homo
Pan

Mots clés :
Locomotion
Diaphyse fémorale
Structure interne
Homo
Pan

ABSTRACT

Within the limits imposed by a number of developmental and rheological factors, endostructural arrangement of the appendicular skeleton is consistent with the functional patterns of stress, where cortical bone topographic thickness variation in long bones primarily reflects the nature, direction, intensity, and frequency of the locomotion-related biomechanical loads. By applying techniques of cross-sectional geometric analysis and 3D morphometric mapping to a (micro)tomographic record consisting of 12 modern human and 10 chimpanzee adult femora, we have shown two distinct patterns (functional "signatures") of cortical bone arrangement along the shaft (20–80% portion of the biomechanical length) specifically associated to the bipedal (*Homo*) and the quadrupedal modes (*Pan*). In particular, the inner structure of the human femoral diaphysis is adapted to anteroposterior loadings and presents a greater rigidity against posterior bending, while that of *Pan* is characterized by the presence of strong medial and lateral bony reinforcements positioned above its femoral midshaft.

RÉSUMÉ

Dans les limites imposées par des contraintes développementales et rhéologiques, l'agencement endostructural du squelette appendiculaire est en adéquation avec les patrons fonctionnels de stress, où les variations topographiques d'épaisseur du tissu cortical des os longs reflètent la nature, la direction, l'intensité et la fréquence des charges biomécaniques en relation avec le mode locomoteur. Grâce à des techniques d'analyse des propriétés géométriques de section et de cartographie morphométrique 3D appliquées au registre (micro)tomographique d'un échantillon de 12 fémurs d'humains modernes et dix de chimpanzés, nous avons mis en évidence deux modèles distincts (« signature » fonctionnelle) d'arrangement de l'os cortical le long de la diaphyse (portion 20–80 % de la longueur biomécanique), spécifiquement en relation à la bipédie (*Homo*) et à la quadrupédie (*Pan*). En particulier, la structure interne de la diaphyse fémorale des humains modernes est adaptée aux contraintes antéropostérieures et présente une grande rigidité contre la flexion postérieure, alors que celle de *Pan* est caractérisée par la présence d'importants renforcements osseux au niveau médial et latéral positionnés au-dessus de la mi-diaphyse.

* Unité d'anthropologie bio-culturelle, « Droit, éthique & santé » (ADÉS), UMR 7268, université d'Aix-Marseille–EFS–CNRS, faculté de médecine – secteur nord, CS 80011, boulevard Pierre-Dramard, 13344 Marseille cedex 15, France.
E-mail address: puymerail@mnhn.fr

1631-0683/$ – see front matter
http://dx.doi.org/10.1016/j.crpv.2013.04.001

1. Introduction

The structure of the postcranial skeleton distinctly reflects intimate aspects of an animal's locomotion (Carter and Beaupré, 2007). Together with the influence on bone shape of genetically-related developmental factors (Lovejoy et al., 1999; Pearson and Lieberman, 2004; Wallace et al., 2010) and some rheological constraints related to the functional response of the osseous material to the usual mechanical stimuli (Ruff et al., 2006; Seeman, 2008), diaphyseal outer and inner structural morphology of the primate appendicular skeleton reflect habitual biomechanical loads primarily related to postural and locomotor modes (Lieberman et al., 2004; Ruff et al., 2006). More specifically, cross-sectional properties provide an estimation of long bone aptitude to resist deformation (Currey, 2002), where cortical bone distribution is largely influenced by locomotor behaviour (Carlson, 2005; Carlson et al., 2006, 2008; Kimura, 2002; Marchi, 2005, 2007; Mazurier et al., 2010; Morimoto et al., 2011a; Ruff and Leo, 1986; Ruff and Runestad, 1992; Ruff et al., 1993, 2006; Seeman, 2008). Accordingly, while some questions concerning the nature of the intimate relationships between the "container" (the cortical shell) and the "contents" (the inner structural organization) remain unresolved (Shaw and Ryan, 2012), the qualitative and quantitative characterization of local morphometric bone properties assessed in long bones potentially provides unique information for reconstructing functionally-related loading histories (Trinkaus and Ruff, 2012).

The reconstruction of postural and locomotor modes from skeletal remains is among the major topics of the paleoanthropological research (e.g., Aiello and Dean, 1990; Fleagle, 1999; Henke and Tattersall, 2007), notably in the case of the earliest representatives of the hominin lineage whose behaviour is still a matter of discussion (Galik et al., 2004; Green and Alemseged, 2012; Lovejoy et al., 1999, 2002, 2009; Pickford et al., 2002; Richmond and Jungers, 2008; White et al., 2009; Wood and Harrisson, 2010). However, in the perspective to perform reliable paleobiomechanical reconstructions based on solid reference models, detailed three-dimensional (3D) measures of site-specific cortical bone organization along the shaft assessed on the locomotory skeleton of extant primate taxa displaying different postural and locomotion patterns are still poorly reported (Bondioli et al., 2010; Morimoto et al., 2011a; Puymerail et al., 2012a, b; Shaw and Ryan, 2012). A 1:1 relationship between locomotion mode, distribution and pattern of activity of the muscle and outer/inner cortical bone structure is still far to be understood in biomechanics (Carter and Beaupré, 2007).

In this exploratory study, we use advanced techniques of 3D functional imaging to comparatively identify, virtually extract and model the features uniquely characterizing the inner structural organization of the adult femoral shaft in two taxa representing distinct locomotory groups among the extant primates: modern humans and chimpanzee (Fleagle, 1999).

Compared to the terrestrial obligatory biped modern humans, chimpanzees mainly travel along the ground using the characteristic knuckle-walking quadrupedal locomotion, but also display a particularly wide range of locomotor-related postures and movements, including vertical climbing, suspensory, bipedalism and scrambling (D'Août et al., 2004; Doran, 1993, 1997; Kivell and Schmitt, 2009; Videan and McGrew, 2001, 2002). Chimpanzee anatomy is found to be generalistic and indicative of an arboreal lifestyle.

Based on the assumption that variation in local morphometric properties of the femoral shaft intimately relates to functional levels and patterns of habitual physical activity, primarily locomotion, we thus expect the combined analysis of cross-sectional geometric properties and morphometric maps run on the two samples respectively provides a distinct "bipedal" and a "quadrupedal" morphostructural signature (Puymerail et al., 2012c).

2. Materials and methods

2.1. The samples

The human sample used in this study consists of 12 adult femora representing two females, seven males and three individuals of unknown sex from 19th-century France ($N = 6$; coll. Musée de l'Homme, Paris, and University of Poitiers) and from the 1st-2nd century Imperial Roman graveyard of Velia, in southern Italy ($N = 6$; coll. Museo Nazionale Preistorico Etnografico "L. Pigorini", Rome).

The chimpanzee (*Pan troglodytes*) sample consists of 10 adult femora from three males, four females and three individuals of unknown sex selected from the African ape skeletal collections stored at the MNHN Paris and the Senckenberg Forschungsinstitut und Naturmuseum, Frankfurt am Main. Unfortunately, information about their original living environment (captive vs. wild) is not systematically available in the files. However, while Jensvold et al. (2001) noted that captive chimpanzees living in confined and less complex environments are characterized by lower locomotor activity, Marchi (2005, 2007) did not find significant differences between captive and wild apes in cross-sectional geometric properties of the tibia, fibula, hand and foot bones This conclusion was recently strengthened by Morimoto et al. (2011a) in their comparative morphometric mapping of the femoral shaft.

Because of the limited number of individuals involved in this preliminary study, data were treated regardless of sex. All material has been selected because of its excellent preservation quality and absence of any macroscopic indication of gross pathology.

2.2. Data acquisition

Femora were scanned using medical computed tomography equipment (CT, $N = 19$) and the synchrotron radiation microtomographer set at the beamline ID 17 of the European Synchrotron Radiation Facility of Grenoble (SR-μCT, $N = 3$). CT-based acquisitions resulted in voxel size ranging from 111 to 710 μm (for the x and y axes), and from 330 to 625 μm (for the z axis), while SR-μCT acquisitions used an isotropic voxel size of 350 μm.

For each femoral specimen, in order to virtually isolate the cortical shell, to image its inner morphology,

and to reconstruct the entire volume, a semi-automatic threshold-based segmentation with manual corrections has been carried out following the half-maximum height method (HMH; Spoor et al., 1993) and the region of interest thresholding protocol (ROI-Tb; Fajardo et al., 2002). On different slices of the virtual stack, repeated measurements (Coleman and Colbert, 2007) have been taken by the Avizo v.6.2. (Visualization Sciences Group Inc.) and ImageJ (Rasband, 2010) packages. The result of the segmentation is a triangulated mesh model of the endosteal and periosteal surfaces composed of 3D coordinate vertices connected by lines that generate triangular faces obtained after "unconstrained smoothing" (Yoo, 2004).

As shown by previous similar studies dealing with long bone 3D virtual modelling using different imaging systems (Bayle et al., 2011; Bondioli et al., 2010; Mazurier et al., 2010; Puymerail, 2011), a number of intra- and interobserver tests for accuracy run by different observers revealed differences less or equal to 5%.

2.3. Cross-sectional geometric properties and morphometric mapping

Two different analytical methods have been used in this analysis in order to characterize the femoral shaft structural organisation in *Homo* and *Pan*: cross-sectional geometry and morphometric mapping (for technical details, see Bondioli et al., 2010). Analyses have been run by means of custom routines developed in Scilab v.5.1.1 (The Scilab Consortium) and in R v.2.12.2 language (R Development Core Team, 2011).

In all investigated cases, cross-sectional geometric properties were assessed on virtual sections set at regular intervals of 1% along the shaft within the portion 20 to 80% of the biomechanical length. Following Ruff (2002), the femoral biomechanical length is measured from the average of the distal condyles to the proximal neck where, by convention, 80% corresponds to the relative proximal end of this shaft portion (thus, 20% is distal). At each cross-sectional level, the following parameters have been systematically measured: total area (TA, in mm^2); cortical area (CA, in mm^2); percent of cortical area (%CA); second moments of area about the medio-lateral (M-L) and antero-posterior (A-P) axes (I*x*, I*y*, in mm^4) and the I*x*/I*y* ratio (see Ruff, 2008; Stock and Shaw, 2007 for further discussion of these properties). To identify behaviourally significant differences in bone structure, it's necessary to control the effects of body size. Since individual body mass values were not available for any specimens of our sample, we choose to specifically focus on the size-free ratio %CA and I*x*/I*y*.

Firstly introduced by Amtmann (1971) and applied to the human fossil record by Zollikofer and Ponce de León (2001, 2005), morphometric mapping is a new way to model stress and strain distribution along the bone shaft (Bondioli et al., 2010; Morimoto et al., 2011a; Puymerail et al., 2012a, b). For the specific purposes of the present study, cortical bone thickness is defined as the distance for each point from a node on the periosteal surface to its closest node on the endosteal surface (Bondioli et al., 2010). Since femoral diaphysis does not significantly deviate from a cylindrical model, the periosteal (external) surface is then mapped into a cylinder whose diameter corresponds to the maximum width of the original shaft surface. By using the (μ)CT-based 3D reconstructions, the cylinder representing each investigated femur is firstly virtually cut vertically along a predefined line along the anterior aspect, and then unrolled into a plane. As the direction of unrolling changes according to the anatomical side of the investigated specimen, it is therefore possible to invert the polarity of this variable in order to obtain fully comparable maps, regardless the original sides.

2.4. Standardization and comparisons

In order to statistically compare for their cortical bone topographic distribution, two samples of femoral shafts representing differently sized and shaped taxa (*Homo* vs. *Pan*), both size of each morphometric map and thickness measurements have been standardized. With special reference to overall size, the 20 to 80% investigated shaft portions have been systematically grid onto a regular mesh of 100 rows by 100 columns. The second step implied thickness standardization between 0 and 1. We then performed a generalized additive modelling (GAM). According to this method, thickness values at the gridline intersections are evaluated by means of thin plate splines regression of the morphometric maps (Wood, 2006). Since morphometric maps fully overlap following standardisation, it is possible to perform GAM in order to obtain distinct consensus maps of the human and the chimpanzee shafts, respectively, by merging all the individual maps into a single dataset (Puymerail, 2011). This protocol allows visual comparative assessments as well as statistical comparisons run by principal component analysis of thickness distribution at the gridline intersections. Two-sample Wilcoxon tests between the two locomotor groups. R v.2.12.2 has been used to run all statistical analysis.

3. Results and discussion

3.1. Cross-sectional geometric properties

The unstandardized values of the cross-sectional geometric properties of the human and chimpanzee femoral samples measured (in distal-proximal direction) at 20%, 35%, 50%, 65% and 80% of the biomechanical length are shown in Table 1, and the scatterplots of the percent of cortical area (%CA) and the I*x*/I*y* ratio (I*x*/I*y*) are presented on Figs. 1 and 2, respectively. In order to simplify the global reading and interpretation of the results, the statistical significance (*P*-values) of the differences at each cross-section for the Wilcoxon test run between the two locomotor groups is provided directly on each scatter plot.

Cortical area (CA) is a measure of strength, rigidity or resistance of the diaphyseal cross-section in pure compression or tension (Lieberman et al., 2004; Ruff, 2008; Sládek et al., 2006). For this variable, differences between *Homo* and *Pan* are evident all along the shaft (Table 1). CA unstandardized values displayed by the human sample used in this study are higher compared to the chimpanzee ones, especially in the proximal portion of the diaphysis (50–80% of the biomechanical length), where humans express

Table 1
Comparative values of the unstandardized geometric properties of the femoral shaft measured in two human ($N = 12$) and chimpanzee ($N = 10$) adult samples at five cross-sectional levels (20%, 35%, 50%, 65% and 80% of the biomechanical length). In italics, the standard deviation (*SD*). See the text (Cross-sectional geometric properties and morphometric mapping) for the meaning of the variables.
Tableau 1
Mesures comparatives des valeurs brutes des paramètres de section mesurés de deux échantillons humains ($N = 12$) et chimpanzés ($N = 10$) à cinq sections (20 %, 35 %, 50 %, 65 % et 80 % de la longueur biomécanique). Les valeurs d'écart-type (*SD*) sont en italique. Voir le texte (*Méthodes*) pour la signification des variables.

(%)		TA	CA	%CA	Ix	Iy	Ix/Iy
20	*Homo* (mean)	862	301	35.1	31 623	43 904	0.68
	SD	*158*	*66*	*6.7*	*10 501*	*15 586*	*0.10*
	Pan (mean)	507	233	44.4	12 213	17 141	0.74
	SD	*75*	*49*	*7.5*	*3324*	*6343*	*0.15*
35	*Homo* (mean)	639	360	55.1	27 630	27 959	0.96
	SD	*108*	*58*	*6.4*	*8632*	*8931*	*0.08*
	Pan (mean)	423	273	61.3	11 799	13 273	0.92
	SD	*48*	*39*	*4.8*	*2538*	*4025*	*0.21*
50	*Homo* (mean)	581	411	75.0	29 366	24 537	1.18
	SD	*91*	*67*	*5.5*	*9178*	*7301*	*0.13*
	Pan (mean)	429	298	66.5	12 808	14 038	0.94
	SD	*45*	*48*	*8.3*	*2896*	*3860*	*0.19*
65	*Homo* (mean)	592	451	78.4	28 054	27 457	1.00
	SD	*98*	*77*	*7.5*	*9062*	*8440*	*0.14*
	Pan (mean)	432	312	68.3	12 783	14 664	0.88
	SD	*48*	*54*	*10.5*	*3230*	*3769*	*0.14*
80	*Homo* (mean)	655	444	67.1	27 788	37 102	0.73
	SD	*108*	*78*	*9.5*	*9464*	*11 562*	*0.12*
	Pan (mean)	453	320	65.8	13 214	16 556	0.79
	SD	*61*	*51*	*9.4*	*3804*	*4273*	*0.10*

CA: cortical area; TA: total area.

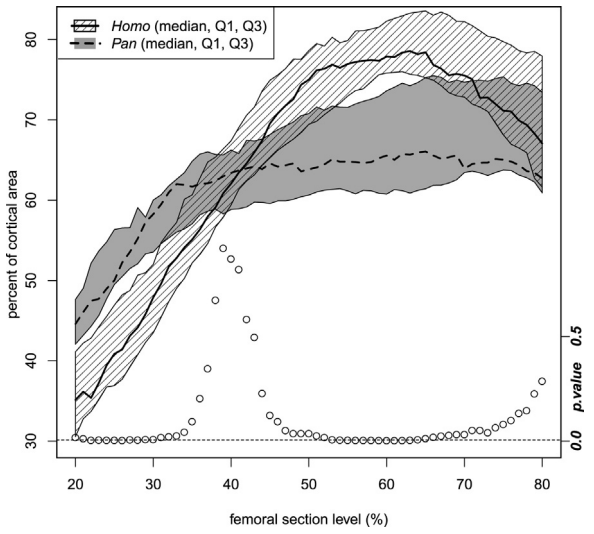

Fig. 1. Percent cortical area (%CA) comparatively measured at regular intervals of 1% along the shaft portion comprised between 20% (distal) and 80% (proximal) of the biomechanical length in modern human (hatched area) and chimpanzee (filled area) femora. Median, first (Q1) and third (Q3) quartile are assessed at each 1% and represent taxonomic variation. Open circles represent *P*-values of the two-sample Wilcoxon test; the horizontal dashed line represents *P*-value = 0.05.
Fig. 1. Pourcentage d'aire corticale mesuré à intervalle régulier de 1 % le long de la portion de la diaphyse fémorale comprise entre 20 % (distal) et 80 % (proximal) de la longueur biomécanique pour le fémur des humains modernes (hachuré) et des chimpanzés (plein). La médiane, le premier (Q1) et le troisième (Q3) quartiles sont calculés à chaque pourcent et représentent la variation taxinomique. Les cercles représentent les valeurs de *p* du test de Wilcoxon et la ligne pointillée horizontale représente $p = 0.05$.

maximum variation. Compared to the human figures, variation in cortical area in our *Pan* sample is globally lower and more uniformly distributed along the shaft. As indicated by Raichlen et al. (2009), compared with other primates, chimpanzees support more weight on their hind limbs because they walk with a relatively protracted hind limb during both terrestrial and arboreal quadrupedalism (Raichlen et al., 2009).

Percent of cortical area (%CA), assessed with respect to the total cross-sectional area (including the medullary cavity), is a measure of diaphyseal resistance in pure compression or tension (Trinkaus and Ruff, 2012). As shown on Fig. 1, *Homo* and *Pan* are clearly distinct for their %CA values in the mid-proximal portion of the femoral diaphysis, notably from 55% to 70% of the biomechanical length. They also differ in the pattern of relative %CA distribution. More specifically, while in chimpanzee the most robust diaphyseal portion is found distally, the opposite is true in the human sample. Furthermore, while %CA values in *Pan* show a marked increase from 20% to 35%, then continuing into a plateau-like outline toward the proximal end, in *Homo* this distal-proximal increase is more accentuated and extends till 55 to 65% of the biomechanical length, where it is followed by a sharp decrease within the remaining shaft portion.

Statistical differences between the two taxa for the Wilcoxon test are significant all along the diaphysis, except for its very proximal portion (70% to 80%) and around 40% of the biomechanical length (Fig. 1). However, it should be also noted that, compared to the modern human figures (Puymerail et al., 2012b, table 3), the site-specific variation at cross-sectional level of cortical thickness assessed along

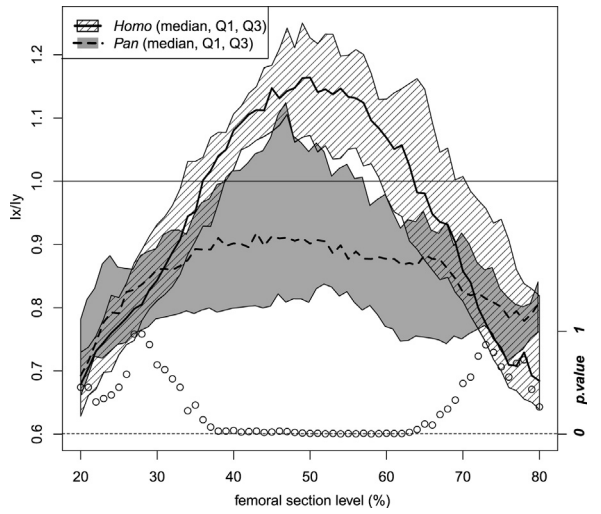

Fig. 2. Values of the I*x*/I*y* ratio comparatively measured at regular intervals of 1% along the shaft portion comprised between 20% (distal) and 80% (proximal) of the biomechanical length in modern human (hatched area) and chimpanzee (filled area) femora. Median, first (Q1) and third (Q3) quartile are assessed at each 1% and represent taxonomic variation. Open circles represent *P*-values of the two-sample Wilcoxon test; the horizontal dashed line represents *P*-value = 0.05.
Fig. 2. Ratio I*x*/I*y* mesuré à intervalle régulier de 1 % le long de la portion de la diaphyse fémorale comprise entre 20 % (distal) et 80 % (proximal) de la longueur biomécanique pour le fémur des humains modernes (hachuré) et des chimpanzés (plein). La médiane, le premier (Q1) et le troisième (Q3) quartiles sont calculés à chaque pourcent et représentent la variation taxinomique. Les cercles représentent les valeurs *p* du test de Wilcoxon et la ligne pointillée horizontale représente $p = 0.05$.

the femoral diaphysis is still poorly reported in adult *Pan* (but see Morimoto et al., 2011a).

The I*x*/I*y* ratio is an index of relative bending strength of the A-P versus M-L bone distribution calculated by using the anatomically oriented second moments of area (Ruff, 2008; Ruff and Hayes, 1983). The outlines shown on Fig. 2 indicate that, with respect to the chimpanzee condition, the human femur is fully adapted to relatively greater M-L bending loads in the proximal and distal shaft portions, and to relatively greater A-P bending loads around the midshaft region (40–60% of the biomechanical length). Conversely, as previously shown by Carlson (2005) in his study of 120 individuals, our results show that the chimpanzee femur is better adapted to relatively greater M-L bending loads all along the diaphysis. Accordingly, the main differences between the two samples for the I*x*/I*y* ratio are found around the midshaft region, while *P*-values of the Wilcoxon test are not significant for the proximal and the distal femoral portions (Fig. 2). Terrestrial and arboreal landscapes are littered with obstacles around which chimpanzees must move; but arboreal locomotion is characterized by multi-directional external forces (Carlson et al., 2006).

Concerning the chimpanzee, the strong variation observed in the biomechanical parameters of the femoral shaft could be explained by variation of sex differences characterizing the locomotor behaviour (e.g., Doran, 1993).

3.2. Morphometric maps

As exemplified by the patterns displayed by two representative specimens respectively selected from the two investigated samples, differences between *Homo* and *Pan* in cortical bone thickness topographic variation for the 20 to 80% portion of the femoral diaphysis are rendered in different anatomical views on Fig. 3. According to this visualisation perspective, marked differences in cortical bone distribution are found on each projection, but the anterior one. However, in order to summarize this spread endostructural variation within a single image of the femoral diaphysis suitable for direct functional comparison, we generated a 3D consensual standardized morphometric map distinctly for the human and the chimpanzee samples (Fig. 4).

The structural signature shown by the modern human map (Fig. 4a) features three major shaft reinforcements. The most developed one corresponds to the posterior pilaster, where the absolutely thickest bone is essentially found around the midshaft. Additional strengthening is recognizable at the level of the proximal medial and the proximal lateral aspects of the shaft, the former representing the structural continuity of the typical asymmetry in cortical bone thickness characterizing the configuration of the bipedally-adapted hominin femoral neck (Galik et al., 2004; Lovejoy et al., 2002; Matsumura et al., 2010; Ohman et al., 1997; Zebaze et al., 2005, 2007). However, while the posterior and the proximal medial features are systematically well expressed in our modern human femora (see also Puymerail et al., 2012a), the degree of development of the lateral thickening is highly variable (cf. Bondioli et al., 2010, fig. 3). This feature consists of two components. Its most distal portion, which is rather anteriorly oriented, is mostly found between 50% and 65% of the biomechanical length, while its proximal portion, between 65% and 80%, is oriented toward the posterior aspect. Together, these structural components roughly correspond to the attachment site of the *gluteus maximus* muscle (Carlson, 2006; Morimoto et al., 2011b; Sigmon, 1974; Swindler and Wood, 1973). In all cases represented in the present study, bone thickening in the modern human femur is distinctly concentrated within the proximal half of the diaphysis, while its distal portion, notably below 35% of the biomechanical length, is relatively and absolutely thin.

In contrast to this pattern, as seen on Fig. 4b, two distinct reinforcements can be identified medially and laterally on the proximal portion of the chimpanzee femoral diaphysis. The former is the most extended one, as it covers the entire medial aspect of the shaft portion between 40% and 80% of the biomechanical length. The lateral one, which is more proximally restricted (70–80%) and corresponds to the lateral spiral pilaster expressed at the external surface of the chimpanzee femur (Morimoto et al., 2011b), commonly appears as a crook-shaped imprint. Finally, a variably expressed posterior bone thickening is occasionally detected in *Pan* between 55% and 65% of the biomechanical length. This structural signature is consistent with the activity and distribution of the thigh muscles of the chimpanzee (Stern and Susman, 1981; Larson and Stern, 2008). As previously noted for *Homo*, the thinnest

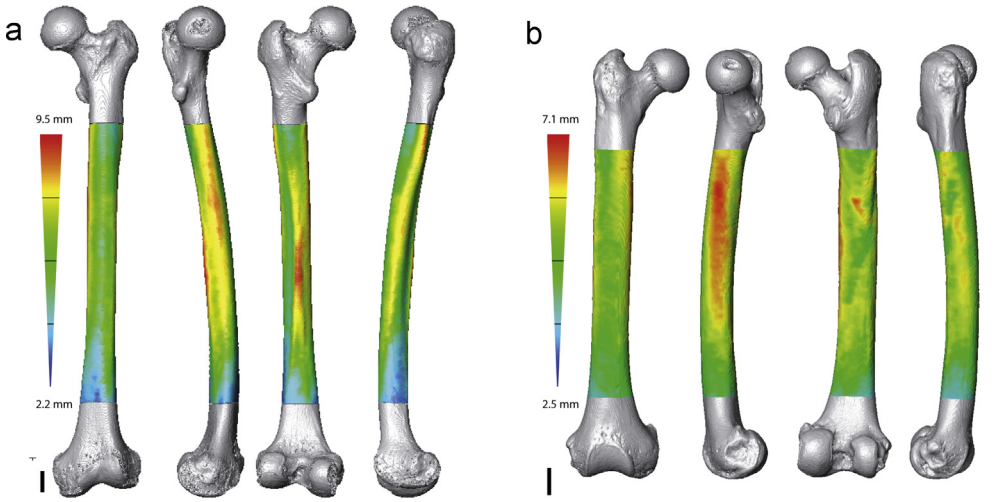

Fig. 3. (μ)CT-based cortical bone thickness topographic distribution assessed for the shaft portion 20 to 80% of the biomechanical length in a human (a) and a chimpanzee (b) femora in (from left to right) anterior, medial, posterior and lateral views. Thickness virtually rendered by a chromatic scale increasing from dark blue to red. Scale bar: 20 mm.

Fig. 3. Reconstruction sur base microtomographique de la distribution topographique des variations d'épaisseur de l'os cortical de la portion de la diaphyse fémorale (20–80 %) d'un humain (a) et d'un chimpanzé (b) représentées (de la gauche vers la droite) en vues antérieure, médiale, postérieure et latérale. Les épaisseurs sont représentées selon une échelle chromatique variant du bleu foncé au rouge. Échelle : 20 mm.

cortical bone along the chimpanzee femoral shaft is again found distally, between 20% and 30% (but see Morimoto et al., 2011a for some structural differences recorded at this level between captive and wild chimpanzees). This functional pattern globally fits the condition described by Morimoto et al. (2011a) following their morphometric analysis based on 16 adult chimpanzee femora.

In order to evidence the most distinct functional areas characterizing the human and chimpanzee diaphyseal pattern, respectively, the individual morphometric maps have been used to run a principal component analysis. Results are shown on Fig. 5.

By representing 30.7% of the total variance, the first component (PC1), which mostly expresses the presence vs. absence of the medial and lateral reinforcements, does not separate humans from chimpanzees. Conversely, a distinction between the two locomotor groups is provided by the second component (PC2, 22.3% of the total variance). In this case, the most discriminant areas in terms of relative cortical bone thickness variation

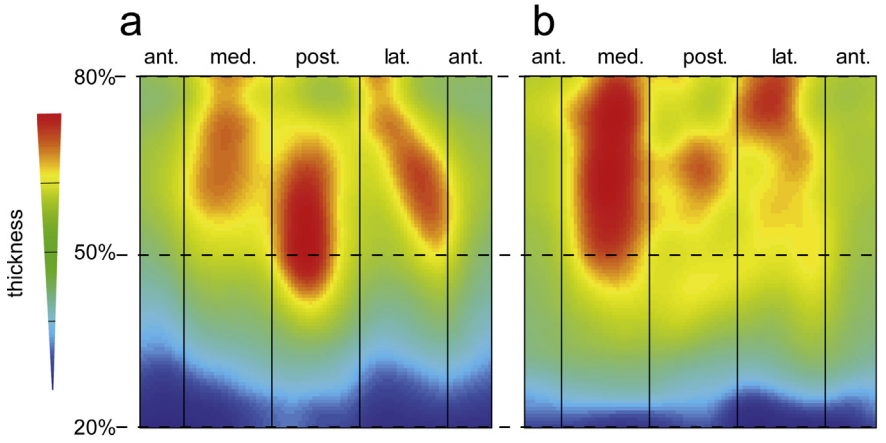

Fig. 4. (μ)CT-based standardized consensual morphometric maps of cortical bone thickness topographic variation assessed for the shaft portion 20 to 80% of the biomechanical length in modern humans (a) and chimpanzee (b). The femora have been virtually unzipped vertically along the middle of the anterior aspect and then unrolled. Imaging perspective is from the inner to the outer surface (medial is to the left). Relative thickness rendered by a chromatic scale increasing from dark blue (0) to red (1).

Fig. 4. Cartographies consensuelles des variations topographiques standardisées de l'os cortical réalisées pour la portion de diaphyse fémorale comprise entre 20 % et 80 % de la longueur biomécanique du consensus des humains modernes (a) et des chimpanzés (b). Les fémurs ont été virtuellement découpés le long de la face antérieure, puis déroulés. Les spécimens sont virtuellement représentés comme gauche ; le point de vue est de l'intérieur vers l'extérieur (côté médial à gauche). Les variations d'épaisseur sont traduites par une échelle chromatique croissante variant du bleu foncé, pour les zones les moins épaisses, au rouge pour les zones les plus épaisses.

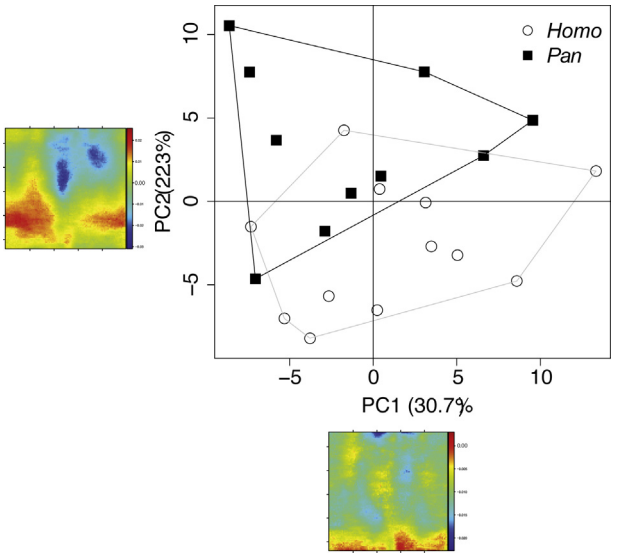

Fig. 5. Principal component analysis of cortical thickness distribution as revealed by individual morphometric maps for the human and chimpanzee femoral samples. Relative contributions along the PC1 and PC2 axes appear at the bottom and to the left of the graph, respectively.
Fig. 5. Analyse en composantes principales de la distribution des épaisseurs corticales décrites par les cartographies morphométriques individuelles des fémurs des échantillons homme et chimpanzé. Les contributions relatives selon la PC1 et la PC2 sont représentées respectivement en dessous et à gauche du graphique.

correspond to the posterior and to the lateral diaphyseal reinforcements, two features which typically characterize the modern human femur. Both regions are found on the proximal half of the shaft, while the distal one is significantly less informative in biomechanical terms. A wilk-lambda test run on the first six components (82.6% of the total variance) reveal highly significant differences between the two groups ($P = 5.56 \times 10^{-6}$, $F = 17.39$). This is in accordance with the proximal attachment onto the femoral shaft of various muscles that are biomechanically relevant for quadrupedalism and bipedalism (Carlson, 2006; Lovejoy et al., 2002; Morimoto et al., 2011b; Sigmon, 1974; Swindler and Wood, 1973). As shown by Thorpe et al. (2009), with the exception of the adductors at the hip, chimpanzees are adapted for more movement at the hindlimb joint than human (Thorpe et al., 2009). At the opposite, human bipedalism requires forces to be exerted with the limbs in particular positions, which are about the same in each stride (Aiello and Dean, 1990). Arboreal locomotor mode generates strains of relatively high magnitude and variable orientation with functional consequences on features of locomotion in general (Carlson, 2005).

4. Conclusions

In this study, we comparatively assessed cortical bone topographic variation along the adult femoral diaphysis in modern humans and chimpanzee in the perspective to recognize two distinct locomotory-related structural signatures. Since we used the same definition of femoral functional length for the two taxa (Ruff and Runestad, 1992), we were able to directly compare the local biomechanical properties across their respective shafts.

As revealed by both cross-sectional geometry and 3D morphometric maps, differences in habitual postural and locomotor modes between *Homo* and *Pan* are clearly reflected in the inner structural organization of their respective femoral diaphysis, bearing unambiguously distinct signatures.

In a functional perspective, which anyhow deserves confirmation through comprehensive analyses based on larger series and also integrating ontogenetic and sex-related variation (e.g., Morimoto et al., 2011a, 2012; Puymerail, 2011), our results mostly show that:

- a locomotion-related functional pattern of site-specific thickness distribution and global endostructural arrangement distinctly characterizes *Homo* and *Pan*. In the samples used for the specific purposes of the present study, main quantitative differences are found in the proximal part of the shaft. This is in accordance with functional concepts that the proximal femur external morphology is directly influenced by pelvic morphology (Ruff, 1995, 2002, 2003; Shaw and Stock, 2011; Trinkaus and Ruff, 2012) and that bending of the proximal human femur reflects evolutionary changes occurred in early hominins in gluteal muscles anatomy and load orientation (Aiello and Dean, 1990; Gibbs et al., 2002; Lovejoy, 2005; Richmond and Jungers, 2008). In particular, opposite to the chimpanzee condition, the human femoral diaphysis is biomechanically stronger proximally for both CA and %CA (Matsumura et al., 2002; Ruff and Runestad, 1992). Additionally, the presence of a fully expressed posterior pilaster is a uniquely derived modern human feature deeply affecting cortical bone distribution pattern across the entire shaft (Cristofolini et al., 1996; De Groote et al., 2010; Ruff, 2002);
- In extant humans, the femur is well adapted to anteroposterior loading and presents a greater rigidity against posterior bending (Puymerail et al., 2012a, b; Ruff, 2002). On the other hand, *Pan* positions its hind limb in a more adducted posture and, notably when moving on arboreal supports, more frequently exerts medially-directed forces (Kivell and Schmitt, 2009; Marchi, 2007; Schmitt, 2003), an evidence which could explain the presence of strong medial and lateral bony reinforcements positioned above its femoral midshaft.

Based on the present preliminary results and the growing evidence from similar independent studies (e.g., Morimoto et al., 2011a, b, 2012), we predict that, once decomposed in their most relevant functional units, the unique "bipedal" and "quadrupedal" morphostructural signatures revealed by means of morphometric mapping of the femoral shaft could be used as proxies to infer postural-locomotor behaviours in studies dealing with the fossil hominid-hominin record (Puymerail, 2011).

Acknowledgements

For access to original osteological material used in the present study, we thank P. Mennecier (Paris),

R. Macchiarelli (Poitiers), V. Volpato (Frankfurt am Main), and L. Bondioli (Rome). E.A. Cabanis (Paris), G. Trainaud (Poitiers) and P. Vandermarcq (Poitiers) allowed access to CT equipments for data recording, and D. Grimaud-Hervé kindly provided help during acquisitions at the CHNO of Paris. A special thank is due to V. Volpato for having realized and generously shared CT analyses of chimpanzee femora in her care. SR-μCT acquisitions at the ESRF of Grenoble have been realized by A. Mazurier (Poitiers). M. Gèze facilitated data elaboration at the MNHN Paris. For support, scientific collaboration and discussion on various aspects of the present and related research on (paleo)biomechanics, we are deeply indebted to G. Berillon (Paris), L. Bondioli, J. Braga (Toulouse), S. Condemi (Marseille), F. Detroit (Paris), M. Friess (Paris), R. Macchiarelli, F. Marchal (Marseille), A. Mazurier, P. O'Higgins (York), B. Richmond (Washington), C.B. Ruff (Baltimore), J. Stock (Cambridge), E. Trinkaus (Chicago), V. Volpato, C. Zanolli (Trieste). The original version benefited from comments from reviewers. Research supported by the MNHN Paris and the French CNRS-INEE.

References

Aiello, L., Dean, C., 1990. An Introduction to Human Evolutionary Anatomy. Academic Press, London, 608 p.

Amtmann, E., 1971. Mechanical Stress, Functional Adaptation and the Variation Structure of the Human Femur Diaphysis. Springer-Verlag, Berlin, 88 p.

Bayle, P., Bondioli, L., Macchiarelli, R., Mazurier, A., Puymerail, L., Volpato, V., Zanolli, C., 2011. Three-dimensional imaging and quantitative characterization of human fossil remains. Examples from the NESPOS database. In: Macchiarelli, R., Weniger, G.C. (Eds.), Pleistocene Databases. Acquisition, Storing, Sharing. Wissenschaftliche Schriften des Neanderthal Museums 4, Mettmann, pp. 29–46.

Bondioli, L., Bayle, P., Dean, C., Mazurier, A., Puymerail, L., Ruff, C., Stock, J.T., Volpato, V., Zanolli, C., Macchiarelli, R., 2010. Technical note: morphometric maps of long bone shafts and dental roots for imaging topographic thickness variation. Am. J. Phys. Anthropol. 142, 328–334.

Carlson, K.J., 2005. Investigating the form-function interface in African apes: relationships between principal moments of area and positional behaviors in femoral and humeral diaphyses. Am. J. Phys. Anthropol. 127, 312–334.

Carlson, K.J., 2006. Muscle architecture of the common chimpanzee (*Pan troglodytes*): perspectives for investigating chimpanzee behavior. Primates 47, 218–229.

Carlson, K.J., Doran-Sheehy, D.M., Hunt, K.D., Nishida, T., Yamanaka, A., Boesch, C., 2006. Locomotor behavior and long bone morphology in individual free-ranging chimpanzees. J. Hum. Evol. 50, 394–404.

Carlson, K.J., Sumner, D.R., Morbeck, M.E., Nishida, T., Yamanaka, A., Boesch, C., 2008. Role of nonbehavioral factors in adjusting long bone diaphyseal structure in free-ranging *Pan troglodytes*. Int. J. Prim. 29, 1401–1420.

Carter, D.R., Beaupré, G.S., 2007. Skeletal Function and Form: Mechanobiology of Skeletal Development, Aging and Regeneration. Cambridge University Press, New York, 332 p.

Coleman, M.N., Colbert, M.W., 2007. Technical note: CT thresholding protocols for taking measurements on three-dimensional models. Am. J. Phys. Anthropol. 133, 723–725.

Cristofolini, L., Viceconti, M., Cappello, A., Toni, A., 1996. Mechanical validation of whole bone composite femur models. J. Biomech. 29, 525–535.

Currey, J.D., 2002. Bones: Structure and Mechanics. Princeton University Press, Oxford, 456 p.

D'Août, K., Vereecke, E., Schoonaert, K., De Clercq, D., Van Elsaker, L., Aerts, P., 2004. Locomotion in bonobos (*Pan paniscus*): differences and similarities between bipedal and quadrupedal terrestrial walking, and a comparison with other locomotor modes. J. Anat. 204, 353–361.

De Groote, I., Lockwood, C.A., Aiello, L., 2010. Technical note: a new method for measuring long bone curvature using 3D landmarks and semi-landmarks. Am. J. Phys. Anthropol. 141, 658–664.

Doran, D.M., 1993. Comparative locomotor behavior of chimpanzees and bonobos: the influence of morphology on locomotion. Am. J. Phys. Anthropol. 91, 83–98.

Doran, D.M., 1997. Ontogeny of locomotion in mountain gorillas and chimpanzees. J. Hum. Evol. 32, 323–344.

Fajardo, R.J., Ryan, T.M., Kappelman, J., 2002. Assessing the accuracy of high-resolution X-ray computed tomography of primate trabecular bone by comparisons with histological sections. Am. J. Phys. Anthropol. 118, 1–10.

Fleagle, J.G., 1999. Primate Adaptation and Evolution. Academic Press, London, 596 p.

Galik, K., Senut, B., Pickford, M., Gommery, D., Treil, J., Kuperavage, A.J., Eckkardt, R.B., 2004. External and internal morphology of the BAR 1002'00 *Orrorin tugenensis* femur. Science 305, 1450–1454.

Gibbs, S., Collard, M., Wood, B., 2002. Soft-tissue anatomy of the extant hominoids: a review and phylogenetic analysis. J. Anat. 200, 3–49.

Green, D.J., Alemseged, Z., 2012. *Australopithecus afarensis* scapular ontogeny, function, and the role of climbing in human evolution. Science 338, 514–517.

Henke, W., Tattersall, I., 2007. Handbook of Paleoanthropology. Springer-Verlag, Berlin, 2069 p.

Jensvold, M.L.A., Sanz, C.M., Fouts, R.S., Fouts, D.H., 2001. Effect of enclosure size and complexity on the behaviors of captive chimpanzees (*Pan troglodytes*). J. Appl. Anim. Welf. Sci. 4, 53–69.

Kimura, T., 2002. Primate limb bones and locomotor types in arboreal or terrestrial environments. Z. Morph. Anthrop. 83, 201–219.

Kivell, T.L., Schmitt, D., 2009. Independent evolution of knuckle-walking in African apes shows that humans did not evolve from a knuckle-walking ancestor. Proc. Natl. Acad. Sci. 106, 14241–14246.

Larson, S.G., Stern, J.T., 2008. Hip extensor EMG and forelimb/hind limb weight support asymmetry in primate quadrupeds. Am. J. Phys. Anthropol. 138, 343–355.

Lieberman, D.E., Polk, J.D., Demes, B., 2004. Predicting long bone loading from cross-sectional geometry. Am. J. Phys. Anthropol. 123, 156–171.

Lovejoy, C.O., 2005. The natural history of human gait and posture. Part 2. Hip and thigh. Gait Post. 21, 113–124.

Lovejoy, C.O., Cohn, M.J., White, T.D., 1999. Morphological analysis of the mammalian postcranium: a developmental perspective. Proc. Natl. Acad. Sci. 96, 13247–13252.

Lovejoy, C.O., Meindl, R.S., Ohman, J.C., Heile, K.G., White, T.D., 2002. The Maka femur and its bearing on the antiquity of human walking: applying contemporary concepts of morphogenesis to the human fossil record. Am. J. Phys. Anthropol. 119, 97–188.

Lovejoy, C.O., Suwa, G., Spurlock, L., Asfaw, B., White, T.D., 2009. The pelvis and femur of *Ardipithecus ramidus*: the emergence of upright walking. Science 326, 71e1–71e6.

Marchi, D., 2005. The cross-sectional geometry of the hand and foot bones of the Hominoidea and its relationship to locomotor behavior. J. Hum. Evol. 53, 647–655.

Marchi, D., 2007. Relative strength of the tibia and fibula and locomotor behavior in hominoids. J. Hum. Evol. 49, 743–761.

Matsumura, A., Takahashi, Y., Okada, M., 2002. Cross-sectional geometric properties along the diaphysis of femur and humerus in chimpanzees and humans. Zeit. Morph. Anthropol. 83, 373–382.

Matsumura, A., Gunji, H., Takahashi, Y., Nishida, T., Okada, M., 2010. Cross-sectional morphology of the femoral neck of wild chimpanzees. Int. J. Prim. 31, 219–238.

Mazurier, A., Nakatsukasa, M., Macchiarelli, R., 2010. The inner structural variation of the primate tibial plateau characterized by high-resolution microtomography. Implications for the reconstruction of fossil locomotor behaviours. C. R. Palevol 9, 349–359.

Morimoto, N., Ponce de León, M.S., Zollikofer, C.P.E., 2011a. Exploring femoral diaphyseal shape variation in wild and captive chimpanzees by means of morphometric mapping: A test of Wolff's law. Anat. Rec. 294, 589–609.

Morimoto, N., Ponce de León, M.S., Nishimura, T., Zollikofer, C.P.E., 2011b. Femoral morphology and femoropelvic musculoskeletal anatomy of humans and great apes: A comparative virtopsy study. Anat. Rec. 294, 1433–1445.

Morimoto, N., Zollikofer, C.P.E., Ponce de León, M.S., 2012. Shared human-chimpanzee pattern of perinatal femoral shaft morphology and its implications for the evolution of hominin locomotor adaptations. Plos One 7, e41980.

Ohman, J.C., Krochta, T.J., Lovejoy, C.O., Mensforth, R.P., Latimer, B., 1997. Cortical bone distribution in the femoral neck of Hominoids: Implications for the locomotion of *Australopithecus afarensis*. Am. J. Phys. Anthropol. 104, 117–131.

Pearson, O.M., Lieberman, D.E., 2004. The aging of Wolff's "law": ontogeny and responses to mechanical loading in cortical bone. Yearb. Phys. Anthrop. 7, 63–99.
Pickford, M., Senut, B., Gommery, D., Treil, J., 2002. Bipedalism in *Orrorin tugenensis* revealed by its femora. C. R. Palevol 1, 191–203.
Puymerail, L., 2011. Caractérisation de l'Endostructure et des Propriétés Biomécaniques de la Diaphyse Fémorale : la Signature de la Bipédie et la Reconstruction des Paléo-Répertoires Posturaux et Locomoteurs des Homininés. PhD dissertation. Muséum national d'Histoire naturelle, Paris, 513 p.
Puymerail, L., Ruff, C.B., Bondioli, L., Widianto, H., Trinkaus, E., Macchiarelli, R., 2012a. Structural analysis of the Kresna 11 *Homo erectus* femoral shaft (Sangiran Java). J. Hum. Evol. 63, 741–749.
Puymerail, L., Volpato, V., Debénath, A., Mazurier, A., Tournepiche, J.F., Macchiarelli, R., 2012b. A Neanderthal partial femoral diaphysis from the "grotte de la Tour", La Chaise-de-Vouthon (Charente France): Outer morphology and endostructural organization. C. R. Palevol 11, 581–593.
Puymerail, L., Bondioli, L., Marchal, F., Macchiarelli, R., 2012c. Functionally-related morphometric maps of femoral cortical bone topographic variation: *Homo vs Pan*. Am. J. Phys. Anthropol. 147 (Suppl. 54), 241.
Raichlen, D.A., Pontzer, H., Shapiro, L.J., Sockol, M.D., 2009. Understanding hind limb weight support in chimpanzees with implications for the evolution of primate locomotion. Am. J. Phys. Anthropol. 138, 395–402.
Rasband, W.S., 2010. ImageJ. US National Institutes of Health, Bethesda, Maryland, USA, http://rsb.info.nih.gov/ij/
Richmond, B.G., Jungers, W.L., 2008. *Orrorin tugenensis* femoral morphology and the evolution of hominin bipedalism. Science 319, 1662–1665.
Ruff, C.B., 1995. Biomechanics of the hip and birth in early *Homo*. Am. J. Phys. Anthropol. 98, 527–574.
Ruff, C.B., 2002. Long bone articular and diaphyseal structure in Old World monkeys and apes I: locomotor effects. Am. J. Phys. Anthropol. 119, 305–342.
Ruff, C.B., 2003. Ontogenetic adaptation to bipedalism: age changes in femoral to humeral length and strength proportions in humans, with a comparison to baboons. J. Hum. Evol. 45, 317–349.
Ruff, C.B., 2008. Biomechanical analyses of archaeological human skeletal samples. In: Katzenberg, M.A., Saunders, S.R. (Eds.), Biological Anthropology of the Human Skeleton, 2nd ed. Wiley-Liss, Hoboken, pp. 183–206.
Ruff, C.B., Hayes, W.C., 1983. Cross-sectional geometry of Pecos Pueblo femora and tibiae – a biomechanical investigation: I. Method and general patterns of variation. Am. J. Phys. Anthropol. 60, 359–381.
Ruff, C.B., Leo, F.P., 1986. Use of computed tomography in skeletal structure research. Yearb. Phys. Anthropol. 29, 181–196.
Ruff, C.B., Runestad, J.A., 1992. Primate limb bone structural adaptations. Ann. Rev. Anthropol. 21, 407–433.
Ruff, C.B., Trinkaus, E., Walker, A.C., Larsen, C.S., 1993. Postcranial robusticity in *Homo* I: Temporal trends and mechanical interpretation. Am. J. Phys. Anthropol. 91, 21–53.
Ruff, C.B., Holt, B., Trinkaus, E., 2006. Who's afraid of the big bad Wolff?: "Wolff's Law"' and bone functional adaptation. Am. J. Phys. Anthropol. 129, 484–498.
Seeman, E., 2008. Modelling and remodelling the cellular machinery responsible for the gain and loss of bone's material and structural strength. In: Bilzezikian, J.P., Raisz, L.G., Rodan, G.A. (Eds.), Principles of Bone Biology. Academic Press, London, pp. 3–28.
Schmitt, D., 2003. Mediolateral reaction forces and forelimb anatomy in quadrupedal primates: implications for interpreting locomotor behavior in fossil primates. J. Hum. Evol. 44, 47–58.
Shaw, C.N., Stock, J.T., 2011. The influence of body proportions on femoral and tibial midshaft shape in hunter-gatherers. Am. J. Phys. Anthropol. 144, 22–29.
Shaw, C.N., Ryan, T.M., 2012. Does skeletal anatomy reflect adaptation to locomotor patterns? Cortical and trabecular architecture in human and nonhuman anthropoids. Am. J. Phys. Anthropol. 147, 187–200.
Sigmon, B.A., 1974. A functional analysis of pongid hip and thigh musculature. J. Hum. Evol. 3, 161–185.
Sládek, V., Berner, M., Sailer, R., 2006. Mobility in central european Late Eneolitic and Early Bronze Age: femoral cross-sectional geometry. Am. J. Phys. Anthropol. 130, 320–332.
Spoor, F., Zonneveld, F., Macho, G.A., 1993. Linear measurements of cortical bone and dental enamel by computed tomography: applications and problems. Am. J. Phys. Anthropol. 91, 469–484.
Stern, J.T., Susman, R.L., 1981. Electromyography of the gluteal muscles in *Hylobates* Pongo, and Pan: implications for the evolution of hominid bipedality. Am. J. Phys. Anthropol. 55, 153–166.
Stock, J.T., Shaw, C.N., 2007. Which measures of diaphyseal robusticity are robust? A comparison of external methods of quantifying the strength of long bone diaphyses to cross-sectional geometric properties. Am. J. Phys. Anthropol. 134, 412–423.
Swindler, D.R., Wood, C.D., 1973. An atlas of primate gross anatomy: baboon, chimpanzee, and man. University of Washington Press, Seattle, 288 p.
Thorpe, S.K.S., Crompton, R.H., Günther, M.M., Ker, R.F., Alexander, R.M., 2009. Dimensions and moment arms of the hind- and forelimb muscles of common chimpanzees (*Pan troglodytes*). Am. J. Phys. Anthropol. 110, 179–199.
Trinkaus, E., Ruff, C.B., 2012. Femoral and tibial diaphyseal cross-sectional geometry in Pleistocene *Homo*. Paleoanthropology, 13–62, http://dx.doi.org/10.4207/PA.2012.ART69.
Videan, E.N., McGrew, W.C., 2001. Are bonobos (*Pan paniscus*) really more bipedal than chimpanzees (*Pan troglodytes*)? Am. J. Prim. 54, 233–239.
Videan, E.N., McGrew, W.C., 2002. Bipedality in chimpanzee (*Pan troglodytes*) and bonobo (*Pan paniscus*): testing hypotheses on the evolution of bipedalism. Am. J. Phys. Anthropol. 118, 184–190.
Wallace, I.J., Middleton, K.M., Lublinsky, S., Kelly, S.A., Judex, S., Garland, T., Demes, B., 2010. Functional significance of genetic variation underlying limb bone diaphyseal structure. Am. J. Phys. Anthropol. 143, 21–30.
White, T.D., Asfaw, B., Beyene, Y., Hailé-Selassié, Y., Lovejoy, C.O., Suwa, G., WoldeGabriel, G., 2009. *Ardipithecus ramidus* and the paleobiology of early hominids. Science 326, 64–86.
Wood, S.N., 2006. Generalized Additive Models: an Introduction with R. Boca Raton. Chapman & Hall, Boca Raton, 410 p.
Wood, B., Harrisson, T., 2010. The evolutionary context of the first hominins. Nature 470, 347–352.
Yoo, T.S., 2004. Insight into images. Principles and practice for segmentation, registration and image analysis. A.K. Peters, Wellesley, 410 p.
Zebaze, R.M.D., Jones, A., Welsh, F., Knackstedt, M., Seeman, E., 2005. Femoral neck shape and the spatial distribution of its mineral mass varies with its size: clinical and biomechanical implications. Bone 37, 234–252.
Zebaze, R.M.D., Jones, A., Knackstedt, M., Maalouf, G., Seeman, E., 2007. Construction of the femoral neck during growth determines its strength in old age. J. Bone Min. Res. 22, 1055–1061.
Zollikofer, C.P.E., Ponce de León, M.S., 2001. Computer-assisted morphometry of hominoid fossil: the role of morphometric maps. In: De Bonis, L., Koufos, G.D., Andrews, P. (Eds.), Hominoid Evolution and Climate Change in Europe. Phylogeny of the Neogene Hominoid Primates of Eurasia. Cambridge University Press, Cambridge, pp. 50–59.
Zollikofer, C.P.E., Ponce de León, M.S., 2005. Virtual Reconstruction: A Primer in Computer-Assisted Paleontology and Biomedicine. J. Wiley & Sons, Inc, Hoboken, 33 p.